

A&A manuscript no.
(will be inserted by hand later)

Your thesaurus codes are:
06 (08.02.3; 08.02.4; 08.02.6; 08.12.2 03.20.7; 08.12.1)

ASTRONOMY
AND
ASTROPHYSICS

Accurate masses of very low mass stars: III 16 new or improved masses. ^{*}

D. Ségransan¹, X. Delfosse², T. Forveille^{1,3}, J.-L. Beuzit^{1,3}, S. Udry⁴, C. Perrier¹ and M. Mayor⁴

¹ Observatoire de Grenoble, 414 rue de la Piscine, Domaine Universitaire de S^t Martin d'Hères, F-38041 Grenoble, France

² Instituto de Astrofísica de Canarias E-38200 La Laguna, Tenerife, Canary Islands, Spain

³ Canada-France-Hawaii Telescope Corporation, P.O. Box 1597, Kamuela, HI 96743, U.S.A.

⁴ Observatoire de Genève, 51 Ch des Maillettes, 1290 Sauverny, Switzerland

Received 21 July 2000, Accepted 28 September 2000

Abstract. We have obtained adaptive optics images and accurate radial velocities for 7 very low mass objects. In the course of a long term effort to determine accurate masses for very low mass stars ($M < 0.6 M_{\odot}$). We use the new data, together with measurements from the literature for some stars, to determine new or improved orbits for these 7 systems. They provide masses for 16 very low mass stars with accuracies that range between 0.2% and 5%, and in some cases a very accurate distance as well. This information is used in a companion paper to discuss the Mass-Luminosity relation for the V, J, H and K photometric bands.

Key words: Stars: binaries - Stars: Binaries spectroscopic - Stars: low mass, brown dwarfs - Techniques: radial velocity - Techniques: adaptive optics

1. Introduction

Accurate masses for binary stars provide a crucial test of our understanding of stellar physics (e.g. Andersen 1991). Mass, the basic input of evolutionary models, is directly measured, and the models must reproduce the effective temperatures and luminosities (or radii) of both components, for a single age and a single chemical composition. Given the strong mass dependency of all stellar parameters however, this discriminating diagnostic only shows its power for relative mass errors $\leq 1-3\%$.

Very accurate mass measurements have long been the exclusive province of double-lined detached eclipsing binaries (Andersen 1991, 1998), for which as a bonus the stel-

lar radii are simultaneously determined. Such systems are however unfortunately rare, and only 44 pairs had yielded masses accurate enough to be included in Andersen 1991's critical compilation, mostly for intermediate mass stars. Relatively few eclipsing binaries have had their masses measured since then. In the mass range of interest here, the literature still contains no more than three well detached eclipsing binaries with substantially subsolar component masses: YY Gem (M0Ve, $0.6+0.6 M_{\odot}$; Bopp 1974; Leung & Schneider 1978), the recently identified GJ 2069A (M3.5Ve, $0.4+0.4 M_{\odot}$; Delfosse et al. 1999a), and CM Dra (M4Ve, $0.2+0.2 M_{\odot}$; Lacy 1977; Metcalfe et al. 1996).

Angularly resolved spectroscopic binaries provide stellar masses in parts of the HR diagram where eclipsing systems are rare or missing, and in particular for very low mass stars. Until recently however, these measurements did not match the $\sim 1\%$ accuracy which can be obtained in detached eclipsing systems. As a consequence, the best representation to date of the empirical M-L relation for M dwarfs had to mostly rely on masses determined with 5-20% accuracy (Henry & McCarthy 1993; Henry et al. 1999). The last two years have seen a dramatic evolution in this respect, with two groups breaking through the former $\sim 5\%$ accuracy barrier. The first group to do so used the 1 mas per measurement astrometric accuracy of the Fine Guidance Sensors (Benedict et al. 1999) on *HST* to determine a few masses of angularly resolved binaries with 2 to 10% accuracy (Franz et al. 1998; Torres et al. 1999; Henry et al. 1999; Benedict et al. 2000). Slightly more recently, we have demonstrated that the combination of very accurate radial velocities with angular separations from adaptive optics imaging can yield masses for VLMS with even better accuracy, of only 1-3% (Forveille et al. 1999; Delfosse et al. 1999b). Here we present 16 new or improved masses determined with the same method, with accuracies that now range between 0.2 and 5%. In a companion paper (Delfosse et al. 2000) we rediscuss the VLMS mass-luminosity relation in the light of these new data. We first discuss the observing program and its sample in Sect. 2 and then present the observations and data pro-

Send offprint requests to: Damien Ségransan, e-mail: segransa@obs.ujf-grenoble.fr

^{*} Based on observations made at the Observatoire de Haute Provence (CNRS), and at the CFH Telescope, operated by the NRCC, the CNRS and the University of Hawaii. Tables 4-15 are available only in electronic form at the CDS via anonymous ftp to cdsarc.u-strasbg.fr (130.79.128.5) or via <http://cdsweb.u-strasbg.fr/Abstract.html>

cessing in Sect. 3. Section 4 describes the orbit adjustment and the mass determination.

2. Observing program

Since 1995 we observe a distance-limited-sample of solar neighbourhood M dwarfs with adaptive optics imaging and high accuracy radial-velocity monitoring (Delfosse et al. 1999c, for a full presentation of the project). This long term effort has two main motivations:

- determine the multiplicity statistics of disk M dwarfs with negligible incompleteness corrections,
- measure very accurate stellar masses.

To specifically address the second goal, we have complemented the main distance limited sample with a few well known M dwarfs binaries, beyond its distance or declination limits. These additional binaries have periods longer than ~ 1 year (shorter period systems beyond a few parsecs are unresolved by 4 meter-class telescopes in the near-IR) and shorter than ~ 10 years (to limit the timescale of the program).

3. Observations and data processing

3.1. Radial-velocity observations

We measure radial-velocities for stars in our sample with the ELODIE spectrograph (Baranne et al. 1996) on the 1.93 m telescope of the Observatoire de Haute Provence (France). This fixed configuration dual-fiber-fed echelle spectrograph covers in a single exposure the 390-680 nm spectral range, at an average resolving power of 42000. An elaborate on-line processing is integrated with the spectrograph control software, and automatically produces optimally extracted and wavelength calibrated spectra, with algorithms described in Baranne et al. (1996). All stars in this programme are observed with a Thorium lamp illuminating the monitoring fiber, as needed for the best ($\sim 10 \text{ m s}^{-1}$) radial-velocity precision. The present paper uses data obtained between September 1995 and April 2000.

A few measurements were also obtained with the CORALIE spectrograph on the recently commissioned 1.2-m Euler telescope at La Silla Observatory (Chile). CORALIE is an improved copy of ELODIE and has very similar characteristics, with the exception of a substantially improved intrinsic stability and a somewhat higher spectral resolution ($R = 50000$).

These spectra are analysed for velocity by numerical cross-correlation with a one-bit (i.e. 0/1) template. This processing is standard for ELODIE spectra (Queloz 1995a, 1995b). The correlation mask used here was derived by Delfosse et al. (1999c) from a high S/N spectrum of Gl 699 (Barnard's stars, M4V). As discussed in Sect. 4, we determine the orbital parameters of double-lined systems

through a direct least square adjustment to the correlation profiles. We recommend that reanalyses of those data similarly use those profiles (available upon request to the authors). For easier reference we nonetheless provide in Table 4 to 10 (only available in the electronic version of this paper) radial velocities for all stars, obtained from adjustment of Gaussian functions to the correlation profiles. The measurement accuracies for the sources discussed here range between 10 and 100 m s^{-1} (depending on apparent magnitude and spectral type), except for the two fastest rotators, GJ 2069 A and YY Gem.

3.2. Adaptive optics imaging

Adaptive optics observations are obtained at the 3.6-meter Canada-France-Hawaii Telescope (CFHT) using PUE'O, the CFHT Adaptive Optics Bonnette (Arsenault et al. 1994, Rigaut et al. 1998) and two different infrared cameras (Nadeau et al. 1994, Doyon et al. 1998). Delfosse et al. (1999c) provide a detailed description of the observing procedure, which we only summarize here.

The program stars are observed in a 4 or 5 positions mosaic pattern, that allows to both determine the sky background from the on-source frames and fully compensate the cosmetic defects of the detector. The science targets are used to sense and correct the incoming wavefront. All of them are bright enough ($R < 14$) to ensure diffraction-limited images in the H and K bands under standard Mauna Kea atmospheric conditions (i.e. for seeing up to $1''$). The corrected point spread function obtained from the AO system is synthesized from simultaneous records of the wavefront sensor measurements and deformable mirror commands, as described by Véran et al. (1997). For pre-1997 observations this ancillary information was not available from the acquisition system, and the point spread function is then instead estimated from observations of a reference single star of similar R-band magnitude. Astrometric calibration fields such as the central region of the Trapezium Cluster in the Orion Nebula (Mc Caughrean & Stauffer 1994), were observed to accurately determine the actual detector plate scale and orientation on the sky.

In good seeing conditions the binaries are observed through J ($1.2 \mu\text{m}$), H ($1.65 \mu\text{m}$) and K ($2.23 \mu\text{m}$) filters, or through corresponding narrow-band filters (usually $[\text{Fe}^+]$ ($1.65 \mu\text{m}$) and $\text{Br}\gamma$ ($2.166 \mu\text{m}$)) for sources which would otherwise saturate the detectors in the minimum available integration time. For worse seeing we restrict observations to the K band, to maintain an acceptable corrected image quality.

We use a deconvolution algorithm (Véran et al. 1999) based on the Levenberg-Marquardt minimisation method and coded within IDL to determine the separation, position angle and magnitude difference between the two stars. With approximate initial values of the positions of the two components along with the PSF reference image, the fit-

Name	Hipparcos	Yale	Soderhjelm	Probst
Gl 234			244.2±2.4	243.2±2.0
YY Gem		74.7±2.5		
GJ 2069A	78.05±5.69			
Gl 644	153.96±4.04	154.8±0.6	155.63±1.81	
Gl 747		122.3±2.5		
Gl 831	124.82±2.88	125.8±2.3		
Gl 866		294.3±3.5		

Table 1. Trigonometric parallaxes used for the orbital adjustment. All values are in mas, the references are Van Altena et al. (1995, Yale); ESA (1997, HIPPARCOS catalog); Probst (1977) and Soderhjelm (1999). The HIPPARCOS value listed for Gl 644 corresponds to its common proper motion companion Gl 643, as the measurement for Gl 644 itself is affected by its unaccounted orbital motion.

ting procedures outputs the flux and pixel coordinates of both stars. The astrometric calibrations then yields the desired angular separations. Table 11 to 15 (only available electronically) list the individual measurements.

Additional angular separations could be obtained from the litterature for some binaries. They are also listed in Table 11 to 15, and discussed in Sect. 4.2 for each relevant system

3.3. Parallaxes

As discussed in Sect. 4, the orbital adjustment can make use of the trigonometric parallax of a multiple system, which is handled as an additional observational constraint on the ratio of its physical and angular dimensions. We have obtained this information (Table 1) from the Yale General Catalog of trigonometric Parallaxes (Van Altena et al., 1995) and the HIPPARCOS catalog (ESA 1997), with some individual entries from Probst (1977) and Soderhjelm (1999).

4. Orbital elements and mass measurements

4.1. Orbital adjustment

All orbits were determined with the ORBIT program (Forveille et al. 1999), through a least square adjustment to all available observations: radial velocities or correlation profiles, angular separations, and trigonometric parallaxes. ORBIT supports triple systems, as well as double ones, as long as three-body effects can be neglected. In the present paper this feature was used for two systems, Gl 644 and Gl866. For double and triple-lined systems we directly adjusted the orbit to the cross-correlation profiles (Forveille et al. 1999, for details), rather than use the radial velocities listed in Table 4 to 10. This significantly improves the accuracy of the orbital parameters, by greatly decreasing the effective number of free parameters of the overall adjustment. This gain is particularly important:

- for triple systems, whose three correlation peaks blend for many velocity configurations,
- for large contrast systems, whose weaker component is sometimes only detected with a low signal-to-noise ratio,
- and for small amplitude pairs, whose peaks remain blended for most of the orbit.

Table 2 lists the orbital elements of the 7 systems for which we obtained a new or significantly improved orbit. Table 3 lists the corresponding orbital parallaxes and masses, whose relative accuracies range between 0.2% and 5%. Fig. 1 and 2 respectively show the individual radial-velocity curves and visual orbits, which we now briefly discuss.

4.2. Individual objects

4.2.1. Gl 234 (Ross 614)

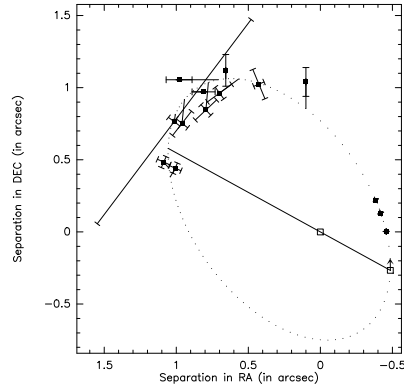
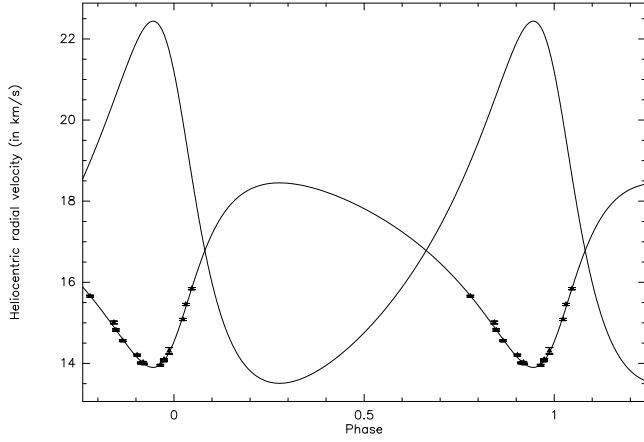
This well known binary is the longest period system ($P = 16.5$ years) for which we obtain a significantly improved orbit, thanks to the availability of early measurements that complement the more accurate data we obtained around the 1999 periastron. The system was initially discovered as an astrometric binary (Reuhl, 1936), and intensively studied as such. Probst (1977) is usually considered as the current reference astrometric orbit. Gl 234 was visually resolved on a few occasions (Lippincott & Hershey, 1972), but its 3.5 magnitude contrast made it a difficult target for visual observers. With the benefit of hindsight, the masses of 0.11 and 0.06 M_{\odot} derived by Probst (1977) turn out to have been underestimated by a large factor. The system was subsequently resolved in speckle observations by Mc Alister & Hartkopf (1988) and Coppenbarger et al. (1994). Coppenbarger et al. (1994) combined these observations with the astrometric orbit of Probst (1977) to derive masses of $M_A = 0.179 \pm 0.047 M_{\odot}$ and $M_B = 0.083 \pm 0.023 M_{\odot}$, compatible within 1σ with the values listed in Table 3.

Our orbit (Table 2) is adjusted to the visual data from Probst (1977), to the 1D and 2D speckle measurements from Coppenbarger et al. (1994), to our more accurate adaptive optics angular separations obtained, to parallaxes from Probst (1977) and Soderhjelm (1999), and to 14 ELODIE radial velocities of the primary (typical accuracy of 50 m/s). The two masses (Table 3) are determined with accuracies of 5.2% for the primary ($0.2027 \pm 0.0106 M_{\odot}$), and 3.4% for the secondary (0.1034 ± 0.0035).

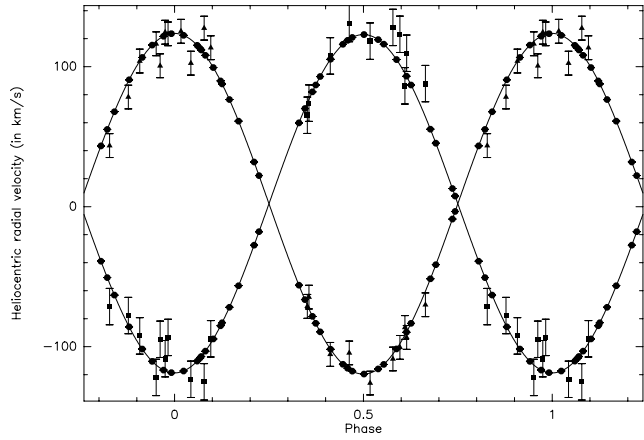
4.2.2. YY Gem

YY Gem is one of the three known detached M-dwarf eclipsing binaries (Bopp 1974, Leung & Schneider 1978). We have obtained 75 radial-velocity measurements of the two components with ELODIE, with typical standard errors of 2 km/s. Both components of YY Gem have their

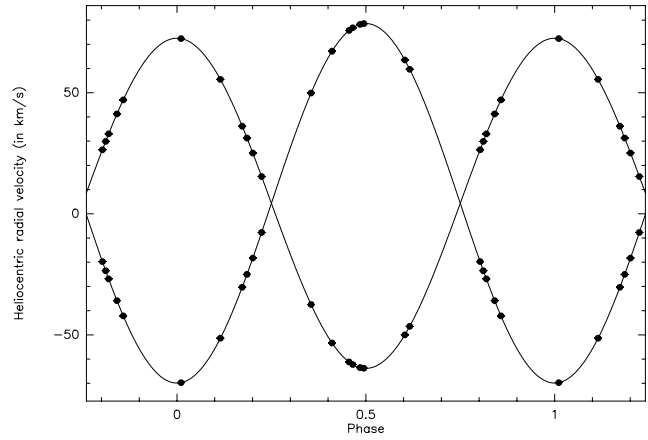
GI 234 (radial-velocity and visual orbit)



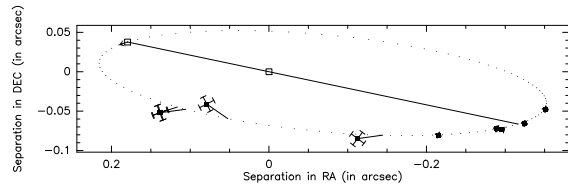
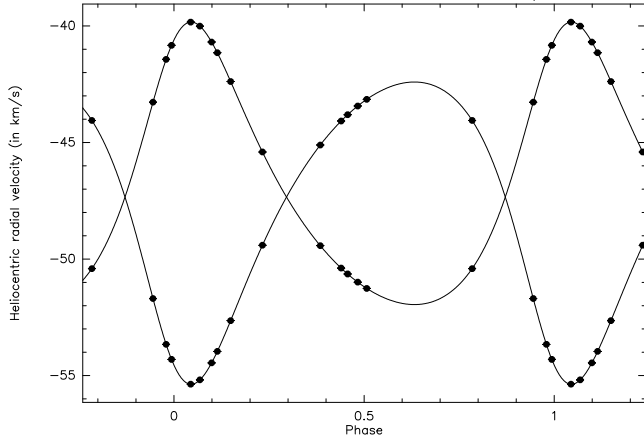
YY Gem (radial-velocity orbit)



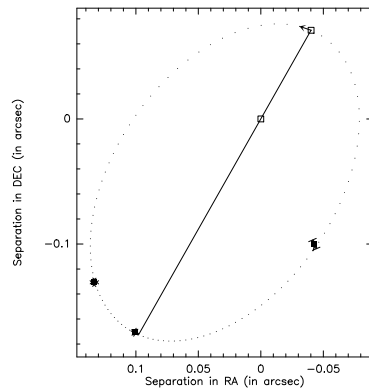
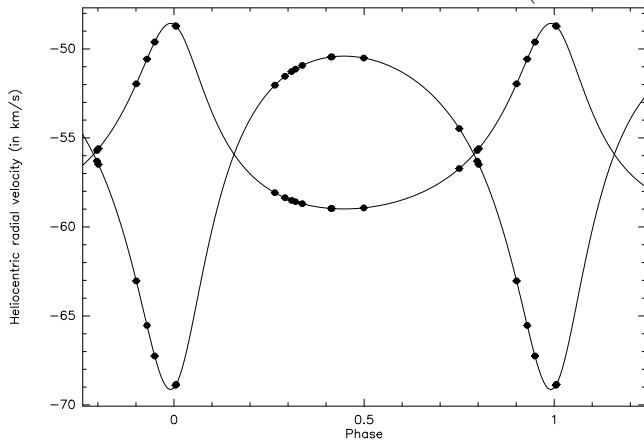
GJ 2069A (radial-velocity orbit)



GI 747 (radial-velocity and visual orbit)



GI 831 (radial-velocity and visual orbit)



Name	P (days)	T ₀ (Modified Julian day)	e	Ω (degree)	ω (degree)	i (degree)	as arc sec	K ₁ (km s ⁻¹)	K ₂ (km s ⁻¹)	V ₀ (km s ⁻¹)
Gl 234AB	5889.0 ±32.	51318. ±13.	.371 ±.004	30.7 ±0.5	223. ±2	51.8 ±0.7	1.04 ±0.01	2.27 ±0.06	4.45 ±0.15	16.79 ±0.06
YY Gem	0.8142818 ±0.0000003	50556.5614 ±0.0004	.0 Fixed			86.5 ±0.05	0.00135 ±0.00005	121.67 ±0.43	120.97 ±0.44	1.97 ±0.24
GJ 2069A	2.771470 ±0.0000012	50579.1907 ±0.0002	.0 Fixed			86.7 ±0.4	0.0028 ±0.0003	68.15 ±0.03	74.24 ±0.05	4.34 ±0.02
Gl 644A-Bab	627.0 ±0.2	53943. ±3.	.042 ±.001	-10.2 ±0.2	306.0 ±1.5	160.3 ±0.1	.2273 ±.0004	5.291 ±0.015	3.33 ±0.02	14.947 ±0.007
Gl 644Ba-b	2.965509 ±0.000006	50919.48 ±0.03	.0209 ±.0008		150. ±3.	164.18 ±0.08		16.73 ±0.02	18.45 ±0.03	
Gl 747AB	2110.0 ±2.5	50432.7 ±1.3	.274 ±.002	85.1 ±0.1	-29.1 ±0.3	77.3 ±0.2	.2881 ±.0005	6.06 ±0.01	6.48 ±0.02	-47.34 ±0.01
Gl 831AB	703.2 ±0.6	50456. ±1.	.416 ±.003	-35.6 ±0.4	8.7 ±0.5	46. ±1.	.1409 ±.0005	5.21 ±0.02	9.4 ±0.1	-55.91 ±0.02
Gl 866AC-B	822.6 ±0.2	51810.3 ±0.4	.439 ±.001	-18.8 ±0.1	158.7 ±0.3	112.6 ±0.1	.3473 ±.0005	5.64 ±0.04	10.43 ±0.04	-50.08 ±0.01
Gl 866A-C	3.786516 ±0.000005	50799.8080 ±0.0005	.0 Fixed			116.5 ±0.5		32.03 ±0.02	40.9 ±0.1	

Table 2. Orbital elements of the newly adjusted orbits. The inclination angles (i) of the two eclipsing binaries, YY Gem and GJ 2069, are fixed to the values derived from analyses of their light curves (from Leung & Schneider 1978 and Delfosse et al. 1999a, respectively). Their other orbital elements are derived from the radial-velocity correlation profiles. All orbital elements of the others stars are simultaneously adjusted to the radial-velocity, parallax, and angular separation data. The inner orbits of Gl 644 and Gl 866 have their inclinations i determined by requiring that the total mass of the inner binary, derived from the outer orbit, must match the sum of the two spectroscopic $M \times \sin^3 i$ obtained from the inner orbit. This leaves an ambiguity between i and $|180 - i|$, which we have tentatively resolved by assuming the approximate coplanarity of their two orbits.

rotation period synchronized with the short orbital period by tidal interactions. The resulting fast equatorial velocities ($v \sin i \sim 30$ km/s) explains this very degraded velocity accuracy. The noisier measurements of Bopp (1974) (~ 10 km/s) are also used in the adjustment and help to constrain the period. The amplitudes, K_1 and K_2 , on the other hand are almost completely determined by the ELODIE measurements, and so are therefore the masses, determined with relative accuracies of 0.2%. We are now obtaining infrared lightcurves of this system to improve the determination of the two stellar radii, and will then present a complete reanalysis.

4.2.3. GJ 2069A (CU Cnc)

GJ 2069A is one of the three known detached M-dwarf eclipsing binaries (Delfosse et al. 1999a). We present here an improved orbit, which includes a few radial-velocity measurements obtained after the completion of Delfosse

et al. (1999a). More importantly, the new orbit was directly adjusted to the ELODIE cross-correlation profiles, whereas our earlier article adjusted an orbit to radial velocities extracted from these profiles. The resulting masses are now among of the most accurate measured for any star (e.g. Andersen 1991, 1998), with 0.2% accuracies for both components. It is somewhat unfortunate that they are not yet matched with equally precise distance, infrared photometry, metallicity, and radii.

We have recently discovered (Beuzit et al., in prep.) a fainter companion to the GJ 2069Aab pair, at a separation of $0.55''$ in early 2000 and which we name GJ 2069D. This makes GJ 2069 a quintuple system, since we had earlier found the fainter visual component, GJ 2069B, to be an adaptive optics and spectroscopic binary (Delfosse et al. 1999c). The new companion is 3 magnitudes fainter than GJ 2069Aab in the K band. Its influence on the photometry can therefore safely be neglected at the current precision of the absolute magnitudes, and the extrapo-

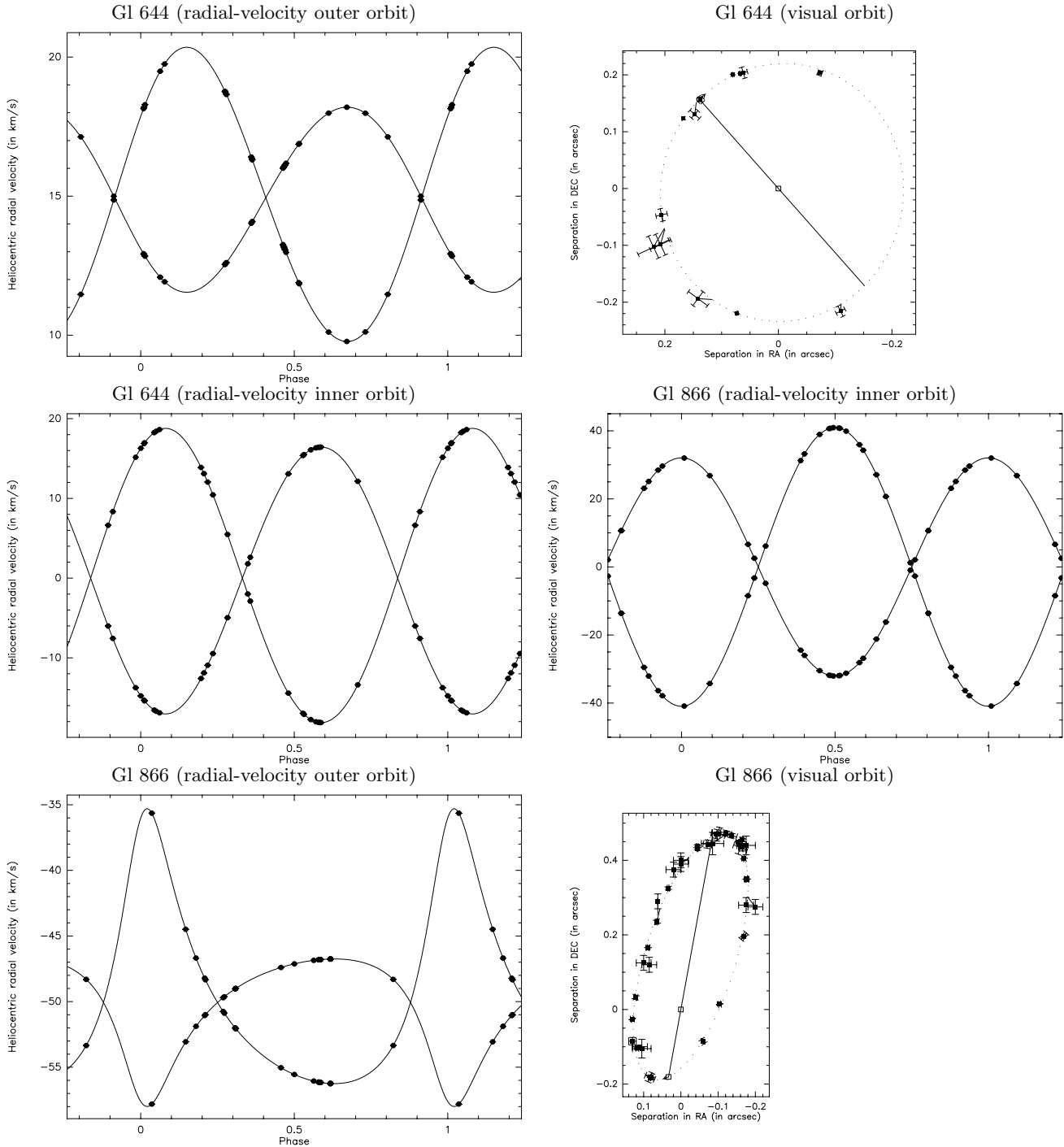


Fig. 2. Radial-velocity and visual orbit for the systems with new or improved mass determinations.

lated luminosity contrast in the V band precludes its detection in the integrated visible spectrum. GJ 2069D will also eventually cause a drift in the systemic velocity of GJ 2069Aab. We have attempted to fit this drift in addition to the parameters of the Aab orbit, but we found that this does not decrease the χ^2 of the adjusted model. This indeterminacy of the drift parameter indicates that the period of the AD system is significantly longer than the ~ 4 years span of the current radial-velocity data. Its

influence does therefore not appreciably bias the measured masses.

4.2.4. Gl 644

At $d = 6.5$ pc, the Gl 644/643 system is the richest stellar system in the immediate solar neighbourhood ($d < 10$ pc), with 5 components Gl 644 (M3V), is the brightest visual component and shares a common proper motion with two

Name		Mass (in M_{\odot})	parallax (in mas)
Gl 234	A	.2027 \pm .0106 (5.2 %)	243.7 \pm 2.0 (0.8%)
	B	.1034 \pm .0035 (3.4%)	
YY Gem	a	.6028 \pm .0014 (0.2%)	
	b	.6069 \pm .0014 (0.2%)	
GJ 2069A	a	.4344 \pm .0008 (0.2%)	
	b	.3987 \pm .0007 (0.2%)	
Gl 644	A	.4155 \pm .0057 (1.4%)	154.8 \pm 0.6 (0.4%)
	Ba	.3466 \pm .0047 (1.3%)	
	Bb	.3143 \pm .0040 (1.3%)	
Gl 747	A	.2137 \pm .0009 (0.4%)	120.2 \pm 0.2 (0.2%)
	B	.1997 \pm .0008 (0.4%)	
Gl 831	A	.2913 \pm .0125 (4.3%)	117.5 \pm 2.0 (1.7%)
	B	.1621 \pm .0065 (4.0%)	
Gl 866	A	.1187 \pm .0011 (0.9%)	293.6 \pm 0.9 (0.3%)
	B	.1145 \pm .0012 (1.0%)	
	C	.0930 \pm .0008 (0.9%)	

Table 3. Masses and parallaxes derived from the orbits listed in Table 2. Except for the two eclipsing systems, the parallaxes represent an optimally weighted combination of the astrometric and orbital parallaxes. Some of them, such as Gl 644, merely reflect the astrometric parallax. Others, such as Gl 866, are almost completely determined by the orbit.

distant companions, Gl 643 (M3.5V) at 72 arc seconds and vB8 (Gl 644C, M7V) at 220 arc seconds. Gl 644 is itself a 1.7-year binary, identified from astrometric observations by Weiss (1982) and Heintz (1984), and first angularly resolved in speckle observations by Blazit et al. (1987) and Tokovinin & Ismailov (1988). Finally, Pettersen et al. (1984) found that one of the two components of Gl 644 (Gl644B) is itself a short period spectroscopic binary, but could not determine its period.

We have obtained 25 ELODIE radial-velocity measurements of Gl 644, which usually appears as a well separated triple-lined system in those data. This allows us to determine for the first time the elements of the inner orbit, whose period is 2.97 days. Such close orbits are very rapidly circularised by tidal interactions. Here we nonetheless measure a small but highly significant eccentricity of $.0209 \pm .0008$. This most likely results from dynamical interactions between the two orbits (Mazeh & Shaham 1979), as could probably be ascertained through a complete dynamical analysis (which would be beyond the scope of the present paper).

The orbital elements listed in Table 2 were simultaneously determined for the two orbits, using angular separation measurements from Blazit et al. (1987), Tokovinin & Ismailov (1988), Al-shukri et al. (1996), Balega et al. (1989, 1991, 1994), Hartkopf et al. (1994), our own more accurate adaptive optics measurements (Table 12), the 25 radial-velocity profiles, and the trigonometric parallaxes of both Gl 644 (Soderhjelm 1999) and Gl 643 (ESA 1997). This determines the masses of all three components with relative accuracies of 1.4 - 1.3%.

This accuracy is obtained even though the orbit is almost seen face-on ($i = 160.3^\circ$), an adverse orientation for accurate mass measurements from radial velocities. ELODIE generally provides very accurate $M \cdot \sin^3(i)$ for double-lined systems, and the mass errors are then typically dominated by the inclination uncertainty. For nearly edge-on orbits, errors on the inclination do not propagate much to $\sin(i)$, and we can then obtain accurate masses even for fairly uncertain inclinations. For nearly face-on orbits on the opposite, one needs a very accurate inclination to determine even moderately accurate masses. Gl 644 demonstrates that we can obtain accurate masses even in some rather poorly oriented orbits.

Interferometric measurements would be needed to resolve the very close inner orbit, but its inclination i_s is nonetheless strongly constrained: $M_{Ba} + M_{Bb}$, as derived from the outer orbit, must match the sum of the two spectroscopic $M \times \sin^3 i_s$ obtained from the inner orbit. This gives $\sin(i_s) = 0.27$, and therefore either $i_s = 164.2^\circ$ or $i_s = 15.8^\circ$. One of those two determinations is very close to the inclination of the outer orbit ($i_s - i_o \sim 4^\circ$). This probably points to a coplanar system, in keeping with a general tendency of close triple systems (Fekel 1981). To ascertain this, one would need to resolve the inner pair, determining Ω_s and obtaining i_s without the reflexion ambiguity.

4.2.5. Gl 747AB (Kui 90)

Gl 747 was first visually resolved in 1936 by Kuiper. Yet, the orbit of this nearby star ($d = 8.5$ pc) has apparently never been determined, probably because its separation never exceeds $0.35''$. It has been resolved in speckle observations once by each of Blazit et al. (1987) and Mc Alister et al. (1987), and three times by Balega et al. (1989). We have complemented these literature measurements with 15 ELODIE radial-velocity profiles of this double-lined system, and 4 separations obtained with PUE'O. The 5.5-year period orbit listed in Table 2 provides an excellent description of all these measurements, with the (strong) exception of the speckle separation obtained by Mc Alister et al. (1987). We could not identify a likely reason for this discrepancy, except that Gl 747 is significantly fainter than most sources in Mc Alister et al. (1987). It could have been close to their sensitivity limit for the conditions under which it was observed, but is on the other hand a system of two equally bright stars. It should therefore not have been an overly difficult target for speckle observations. We have chosen to ignore this data point, since all other measurements are mutually consistent to within approximately their stated standard errors, and since some of them have been observed within a year of the discrepant point. This orbit determines the masses of the two components ($2 \times 0.2 M_{\odot}$) with an accuracy of $\sim 0.4\%$, and the orbital parallax with a 0.2 mas standard error. The latter is in excellent agreement with the less precise astrometric parallax listed in Van Altena et al. (1995).

4.2.6. Gl 831

Gl 831 was first noticed as a P=1.93-year astrometric binary (Lippincott 1979, Mc Namara et al. 1987), and then resolved by visible speckle observations (Blazit et al. 1987). It appears in ELODIE observations as a double-lined spectroscopic binary, but the contrast between the two peaks of the correlation function is large (~ 10) and most of the time their separation is not very much larger than their combined width. It is therefore a good illustration of the improvement brought by a direct adjustment of the orbit to the correlation profiles. Using three adaptive optics angular separations, the parallax from Van Altena et al. (1995) and 14 ELODIE correlation profiles we determine both masses with 4% relative accuracy.

Henry et al. (1999) have found tentative evidence for a third component of Gl 831 in their *HST* FGS observations of this system. This companion would be ~ 3 magnitude fainter in the V band than the primary, and it could be either very close to A or B, or beyond $\sim 0.5''$. We can now firmly exclude the first possibility for a physical member of Gl 831: it would necessarily imply very large velocity variations of the corresponding bright component. A red companion that is only three magnitude fainter in the V band than the primary would be easily detected in our K band adaptive optics images, unless it was always fortuitously within $\sim 0.15''$ of the primary or within $0.1''$ of Gl 831B, whenever we observed it. As this is rather unlikely, the companion, if real, is most likely bluer than Gl 831. It could then either be a white dwarf member of the system, or an unrelated background object.

4.2.7. Gl 866

We recently (Delfosse et al. 1999b) discussed in detail this system of three very low mass stars ($3 \times \sim 0.1 M_{\odot}$), and obtained individual masses with $\sim 3\%$ accuracy. Shortly thereafter Woitas et al. (2000) published a large set of new angular separation measurements. Lacking radial-velocity information, they could only obtain the total mass of the system, with $\sim 10\%$ accuracy. We analyse here the combination of the two datasets, and obtain a very substantial improvement over either of these previous analyses. All three masses are now determined with $\sim 1\%$ accuracy. Gl 866C, the faintest member of the system, is the only star with a dynamically determined mass ($0.0930 \pm 0.0008 M_{\odot}$) that is safely lower than $0.1 M_{\odot}$.

5. Conclusions

We have presented here mass measurements for 16 VLMS, with accuracies which range between 0.5 and 5%, and for masses down to below $0.1 M_{\odot}$. We will shortly publish a few additional masses whose derivation involve long baseline interferometric measurements (Ségransan et al., in prep.). These results only represent a snapshot of the

progress of our mass measurement program: we continue to monitor the VLMS binaries with high accuracy radial-velocity observations and adaptive optics imaging, and have started using long baseline interferometry. Most of the masses which we present here will be improved in the future, and additional ones with similar accuracies will become available.

In a companion paper (Delfosse et al. 2000), we show that these masses provide an impressive validation of the theoretical infrared M-L relations of Baraffe et al. (1998), but point towards low level (~ 0.5 mag) deficiencies of these models in the V band.

A logical next step for this type of work is the determination of accurate masses for even fainter objects, the very late M dwarfs and the L dwarfs. There is at present a large effort in determining the mass function across the stellar/substellar boundary in young open clusters (Bouvier et al. 1998, Zapatero Osorio et al., in prep.) and in the field (Reid et al. 1999, Delfosse & Forveille 2000). These programs need an accurate calibration of the mass as a function of both luminosity and age (due to the dominant effect of cooling for brown dwarfs). Up to now such relations are only available from models, which unfortunately meet with new difficulties for temperatures lower than were relevant in this paper, as dust condenses in the atmospheres of very cool dwarfs.

Until very recently, no binary of such mass was known with a period short enough for a mass determination over any realistic time scale. A few are now known (Martín et al. 1999, 2000, Koerner et al. 1999), even though their periods are either shorter or longer than would be ideal for a quick and accurate mass measurement. They will eventually provide mass determinations for brown dwarfs, but additional efforts to find more brown dwarfs binaries, and better suited ones, are certainly more than warranted. Several groups are doing this, following up the late-M and L dwarfs discovered by the SLOAN, 2MASS and DENIS surveys.

Acknowledgements. We thank the technical staff and telescope operators of OHP and CFHT for their efficient support during these long-term observations. This research has made use of the Simbad database, operated at CDS, Strasbourg, France, of the WDS catalog maintained at the USNO, Washington, USA, and of the Third Catalog of Interferometric Measurements of Binary Stars.

References

- Al-Shukri A.M., McAlister H.A., Hartkopf W.I., Hutter D.J., Franz O.G, 1996, AJ 111, 393
- Andersen J., 1991, Astronomy and Astrophysics Review 3, 91
- Andersen J., 1998, p. 99 in Fundamental Stellar Properties: The Interaction between Observations and Theory, IAU Colloquium 189, T. R. Bedding et al., Eds., Kluwer: Dordrecht

- Arsenault R., Salmon D., Kerr J., et al., 1994, in SPIES Proceedings 2201, “Adaptive Optics in Astronomy”, eds. M.A. Ealey, F. Merkle, 833
- Balega I.I., Balega Yu.Yu., Vasyuk V.A., 1989, *Astrofiz. Issled. Izv. Spets. Astrofiz. Obs.* 28, 107
- Balega I.I., Balega Yu.Yu., Vasyuk V.A. 1991, *Astrofiz. Issled., Izvestia Spets. Astrofiz. Obs.* 31, 80
- Balega I.I., Balega Yu.Yu., Belkin I.N., et al., 1994, *A&AS* 105, 503
- Baraffe I., Chabrier G., Allard F., Hauschildt P.H., 1998, *A&A* 337, 403
- Baranne A., Queloz D., Mayor M., et al. 1996, *A&AS* 119, 373
- Benedict G.F., McArthur B.E, Chappell D.W., et al., 1999, *AJ* 118, 1086
- Benedict G.F., McArthur B.E., Franz O.G., Wasserman L.H., Henry T.J., 2000, *AJ* in press
- Blazit A., Bonneau D., Foy R., 1987, *A&ASS* 71, 57
- Bopp B.W. 1974, *ApJ* 193, 389
- Bouvier J., Stauffer J. , Martín E.L., et al., 1998, *A&A* 336, 490
- Coppenbarger D.S., Henry T.J., Mc Carthy Jr D.W., 1994, *AJ* 107, 1551
- Delfosse X., Forveille T., Mayor M., Burnet M., Perrier C., 1999a, *A&A* 341, L63
- Delfosse X., Forveille T., Udry S., et al., 1999b, *A&A* 350, L39
- Delfosse X., Forveille T., Beuzit J.-L., et al., 1999c, *A&A* 344, 897
- Delfosse X., Forveille T., Ségransan D., et al., 2000, *A&A* in press
- Delfosse X., Forveille T., 2000, in “Very low-mass star and brown dwarfs in stellar clusters and associations”, Eds. Rebolo R., Zapatero Osorio M. R., Bejar V., Cambridge University Press (CUP), in press
- Doyon R., Nadeau D., Vallee P., et al., 1998, in SPIE Proceedings 3354, “Infrared Astronomical Instrumentation”, ed. A.M. Fowler, 760
- ESA, 1997, The HIPPARCOS Catalogue, ESA SP-1200
- Fekel F. C., 1981, *ApJ* 246, 879
- Forveille T., Beuzit J.-L., Delfosse X., et al., 1999, *A&A* 351, 619
- Franz O.G., Henry T.J., Wasserman L.H., et al., 1998, *AJ* 116, 1432
- Hartkopf W.I., McAlister H.A., Mason B.D., et al., 1994, *AJ* 108, 2299
- Heintz W. D., 1984, *PASP* 96, 439
- Henry T.J., McCarthy Jr D.W., 1993, *ApJ* 350, 334
- Henry T.J., Franz O.G., Wasserman L.H., et al., 1999, *ApJ* 512, 864
- Koerner D.W., Kirkpatrick J.D., McElwain M.W., Bonaventure N.R., 1999, *ApJ* 526, L25
- Lacy C.H., 1977, *ApJ* 218, 444
- Leinert C., Haas M., Allard F., et al. 1990, *A&A* 236, 399
- Leung K.C., Schneider D.P., 1978, *AJ* 94, 712
- Lippincott S.L., 1979, *PASP* 91, 784
- Lippincott S.L., Hershey J.L., 1972, *AJ* 77, 679
- McAlister H.A., Hartkopf W.I., Hutter D.J., Franz O.G., 1987, *AJ* 93, 688
- McAlister H. A., Hartkopf W. I., 1988, Second Catalog of Interferometric Measurements of Binary Stars, CHARA contribution No. 2
- McCaughrean M.J., Stauffer J.R., 1994, *AJ* 108, 1382
- McNamara B.R., Ianna P.A., Fredrick L.W., 1987, *AJ* 93, 1245
- Martín E.L., Brandner W., Basri G., 1999, *Science* 283, 1718
- Martín E.L., Koresko C.D., Kulkarni S.R., Lane B.F., Wizinowich P.L., 2000, *ApJ* 528, L37
- Mazeh T. and Shaham J., 1979, *A&A* 77, 145
- Metcalfe T.S., Mathieu R.D., Latham D.W., Torres G., 1996, *ApJ* 456, 356
- Nadeau D., Murphy D.C., Doyon R., Rowlands N., 1994, *PASP* 106, 909
- Pettersen B.R., Evans D.S., Coleman L.A., 1984, *ApJ* 282, 214
- Probst R. G., 1977, *AJ* 82, 656
- Queloz D., 1995a, PhD Thesis 2788, University of Geneva
- Queloz D., 1995b, in IAU Symposium 167, “New developments in array technology and applications”, ed. A.G. Davis Philip (Dordrecht: Kluwer), 221
- Reid I.N., Kirkpatrick J.D., Liebert J., et al., 1999, *ApJ* 521, 613
- Reuhl D., 1936, *AJ* 45, 133
- Rigaut F., Salmon D., Arsenault R., et al., 1998, *PASP* 110, 152
- Schroeder D.J., Golimowski D.A., Brukardt R.A., et al., 2000, *AJ* 119, 906
- Soderhjelm S., 1999, *A&A* 341, 121
- Tokovinin A.A., Ismailov R.M., 1988, *A&ASS* 72, 563
- Torres G., Henry, T.J., Franz O.G., Wasserman L.H., 1999, *AJ* 117, 562
- Van Altena W.F., Lee J.T., Hoffleit D., 1995, The General Catalogue of Trigonometric Stellar Parallaxes, Fourth edition, Yale University Observatory
- Véran J.-P., Rigaut F., Rouan D., Maitre H., 1997, *J. Opt. Soc. Am. A* 14(11), 3057
- Véran J.-P., Beuzit J.-L., Chaytor D., 1999, in “Astronomy with adaptive optics : present results and future programs”, Ed. D. Bonaccini, ESO Conference and Workshop Proceedings, vol. 56, 691
- Weiss E.W., 1982, *AJ* 87, 152
- Woitats J., Leinert Ch., Jahreiss H., et al., 2000, *A&A* 353, 253

Gl234AB

Julian Day 2400000+	V_A (in km/s)	Reference
		this paper
50018.6620	$15.658 \pm .050$	
50388.6449	$15.007 \pm .050$	
50418.5618	$14.824 \pm .050$	
50524.3498	$14.557 \pm .050$	
50747.6659	$14.204 \pm .050$	
50803.5423	$14.010 \pm .050$	
50838.4212	$14.025 \pm .050$	
50851.3844	$13.989 \pm .050$	
51107.6827	$13.955 \pm .050$	
51159.5379	$14.071 \pm .050$	
51163.6391	$14.096 \pm .050$	
51243.3511	$14.310 \pm .080$	
51455.6608	$15.083 \pm .050$	
51500.5519	$15.452 \pm .050$	
51509.6176	$15.322 \pm .050$	
51594.3558	$15.843 \pm .050$	

Table 4. Radial-velocity measurement of Gl 234A. To be published in electronic form only.

YY Gem

Julian Day 2400000+	V_A (in km/s)	V_B (in km/s)	Reference
			Bopp 1974
40988.819000	121.800000 ± 8.500000	-86.100000 ± 13.00000	
40991.858000	51.900000 ± 8.500000	-63.100000 ± 13.00000	
40992.792000	132.900000 ± 8.500000	-100.300000 ± 13.00000	
40992.876000	135.800000 ± 8.500000	-116.800000 ± 13.00000	
40995.741000	-92.200000 ± 8.500000	131.400000 ± 13.00000	
40995.796000	-61.800000 ± 8.500000	96.200000 ± 13.00000	
40996.784000	86.600000 ± 8.500000	-69.500000 ± 13.00000	
40996.844000	124.600000 ± 8.500000	-113.700000 ± 13.00000	
40998.802000	-56.300000 ± 8.500000	82.200000 ± 13.00000	
40998.848000	-97.200000 ± 8.500000	116.000000 ± 13.00000	
40999.827000	-85.100000 ± 8.500000	117.900000 ± 13.00000	
41285.879000	112.300000 ± 8.500000	-84.000000 ± 13.00000	
41285.923000	108.900000 ± 8.500000	-86.400000 ± 13.00000	
41285.968000	133.600000 ± 8.500000		
41292.845000	-96.200000 ± 8.500000	139.100000 ± 13.00000	
41292.890000	-117.700000 ± 8.500000	126.500000 ± 13.00000	
41292.939000	-100.500000 ± 8.500000	136.300000 ± 13.00000	
41292.965000	-78.000000 ± 8.500000	94.600000 ± 13.00000	
41343.754000	131.700000 ± 8.500000	-85.100000 ± 13.00000	
41345.683000	-62.900000 ± 8.500000	73.600000 ± 13.00000	
41348.689000	110.800000 ± 8.500000	-115.000000 ± 13.00000	
			This paper
50386.658000	-68.060000 ± 2.000000	71.317000 ± 2.010000	
50388.689000	65.666000 ± 2.000000	-61.937000 ± 2.000000	
50389.564000	106.155000 ± 2.000000	-101.269000 ± 2.010000	
50389.682000	114.474000 ± 2.000000	-106.669000 ± 2.010000	
50389.691000	111.486000 ± 2.000000	-104.108000 ± 2.010000	
50419.603000	45.879000 ± 2.000000	-39.742000 ± 2.010000	
50420.679000	88.566000 ± 4.000000	-82.566000 ± 4.000000	
50803.603000	-93.102000 ± 2.000000	94.896000 ± 2.010000	
50803.662000	-114.114000 ± 2.000000	117.833000 ± 2.010000	
50804.466000	-111.310000 ± 2.000000	115.248000 ± 2.010000	
50804.512000	-122.679000 ± 2.000000	122.554000 ± 2.010000	
50804.554000	-111.279000 ± 2.000000	114.730000 ± 2.010000	
50804.613000	-87.933000 ± 2.000000	88.354000 ± 2.010000	
50804.655000	-48.587000 ± 2.000000	55.073000 ± 2.010000	
50804.702000	-12.103000 ± 5.000000	19.282000 ± 5.000000	
50837.280000	-8.535000 ± 5.000000	15.242000 ± 5.000000	
50837.344000	53.059000 ± 2.000000	-48.892000 ± 2.010000	
50837.441000	114.356000 ± 2.000000	-110.317000 ± 2.010000	
50837.482000	123.220000 ± 2.000000	-120.601000 ± 2.010000	
50837.544000	111.180000 ± 2.000000	-107.552000 ± 2.010000	
50837.573000	99.324000 ± 2.000000	-93.619000 ± 2.010000	
50837.607000	76.596000 ± 2.000000	-72.885000 ± 2.010000	
50837.671000	27.926000 ± 4.000000	-21.195000 ± 4.000000	
50838.279000	121.265000 ± 2.000000	-119.862000 ± 2.010000	
50838.323000	120.991000 ± 2.000000	-119.629000 ± 2.010000	
50838.370000	106.760000 ± 2.000000	-101.976000 ± 2.010000	
50838.402000	91.200000 ± 2.000000	-86.156000 ± 2.010000	
50838.441000	56.558000 ± 2.000000	-53.281000 ± 2.010000	
50838.475000	34.583000 ± 3.000000	-29.543000 ± 3.000000	
50838.571000	-55.664000 ± 2.000000	57.430000 ± 2.010000	
50838.601000	-77.094000 ± 2.000000	85.060000 ± 2.010000	
50839.422000	-85.943000 ± 2.000000	90.506000 ± 2.010000	
50839.454000	-101.098000 ± 2.000000	105.197000 ± 2.010000	
50839.501000	-119.696000 ± 2.000000	121.266000 ± 2.010000	
50839.557000	-117.400000 ± 2.000000	118.909000 ± 2.010000	
50839.618000	-91.110000 ± 2.000000	93.943000 ± 2.010000	
50839.681000	-39.312000 ± 2.000000	45.560000 ± 2.010000	

Table 5. Radial-velocity measurements of YY Gem. To be published in electronic form only.

GJ2069A

Julian Day 2400000+	V_A (in km/s)	V_B (in km/s)	References
			this paper
50102.528000	72.363000 ± 0.387000	-70.039000 ± 0.671000	
50180.417000	55.762000 ± 0.387000	-51.727000 ± 0.671000	
50181.389000	-62.507000 ± 0.387000	76.540000 ± 0.671000	
50181.442000	-63.163000 ± 0.387000	78.303000 ± 0.671000	
50182.323000	26.906000 ± 0.387000	-20.842000 ± 0.671000	
50182.369000	33.245000 ± 0.387000	-26.164000 ± 0.671000	
50182.430000	41.317000 ± 0.387000	-37.358000 ± 0.671000	
50182.476000	46.551000 ± 0.387000	-42.814000 ± 0.671000	
50183.384000	31.521000 ± 0.387000	-23.989000 ± 0.671000	
50183.427000	25.212000 ± 0.387000	-18.244000 ± 0.671000	
50183.491000	16.000000 ± 0.387000	-8.064000 ± 0.671000	
50228.354000	-53.128000 ± 0.387000	67.222000 ± 0.671000	
50231.357000	-62.646000 ± 0.387000	79.392000 ± 0.671000	
50389.667000	-46.490000 ± 0.200000	59.689000 ± 0.300000	
50525.433000	-50.097000 ± 0.200000	63.745000 ± 0.300000	
50921.344000	-61.063000 ± 0.200000	75.378000 ± 0.300000	
50922.330000	29.951000 ± 0.200000	-23.427000 ± 0.300000	
50923.332000	36.079000 ± 0.200000	-30.010000 ± 0.300000	

Table 6. Radial-velocity of measurements of GJ 2069A. To be published in electronic form only.

Gl644ABC

Julian Day 2400000+	V_A (in km/s)	V_B (in km/s)	V_C (in km/s)	References
				this paper
50182.632800	10.129 ± 0.2	33.141 ± 0.1	0.882 ± 0.1	
50228.466500	11.377 ± 0.3	3.207 ± 0.3	32.846 ± 0.1	
50522.682700	18.770 ± 0.1	-0.128 ± 0.1	26.453 ± 0.5	
50523.677200	18.775 ± 0.1	28.264 ± 0.1	-4.916 ± 0.1	
50525.676200	18.770 ± 0.1	0.709 ± 0.1	25.831 ± 1.0	
50577.575700	16.250 ± 0.2	25.700 ± 0.2	0.776 ± 0.1	
50578.575200	16.253 ± 0.1	-2.642 ± 0.1	32.580 ± 0.1	
50641.367100	13.100 ± 0.1	5.449 ± 0.1	28.058 ± 0.1	
50642.363200	13.138 ± 0.1	32.297 ± 0.1	-1.761 ± 0.1	
50642.450100	13.170 ± 0.1	32.563 ± 0.1	-2.097 ± 0.1	
50643.370600	13.100 ± 0.2	10.585 ± 0.2	21.862 ± 0.3	
50644.383200	13.100 ± 0.1	6.955 ± 0.1	26.544 ± 0.12	
50645.402500	13.007 ± 0.1	32.658 ± 0.1	-2.013 ± 0.1	
50647.489500	13.100 ± 0.1	11.551 ± 0.3	21.004 ± 0.3	
50673.342200	11.840 ± 0.2	2.608 ± 0.2	33.383 ± 0.1	
50674.375400	11.840 ± 0.2	18.198 ± 0.7	15.992 ± 0.7	
50922.626000	14.963 ± 0.1	-2.053 ± 0.1	33.717 ± 0.15	
50983.445800	18.133 ± 0.1	29.089 ± 0.15	-5.269 ± 0.1	
50986.460400	18.221 ± 0.1	29.203 ± 0.1	-5.425 ± 0.1	
51017.372300	19.600 ± 0.25	-3.340 ± 0.1	28.400 ± 1.0	
51026.368200	19.428 ± 0.15	-4.932 ± 0.1	28.943 ± 0.6	

Table 7. Radial-velocity measurements of Gl 644ABC. To be published in electronic form only.

GI747AB

Julian Day 2400000+	V_A (in km/s)	V_B (in km/s)	References
			this paper
49977.364600	-50.669 ± 0.300	-44.148 ± 0.300	
50316.358000	-43.284 ± 0.028	-51.687 ± 0.033	
50389.276800	-41.424 ± 0.040	-53.637 ± 0.048	
50419.282000	-40.684 ± 0.072	-54.347 ± 0.089	
50525.626700	-39.752 ± 0.037	-55.393 ± 0.044	
50576.609400	-39.877 ± 0.056	-55.123 ± 0.068	
50641.514600	-40.692 ± 0.025	-54.390 ± 0.032	
50673.400000	-41.078 ± 0.022	-53.917 ± 0.025	
50747.277800	-42.416 ± 0.040	-52.784 ± 0.040	
50923.634600	-46.246 ± 0.500	-49.668 ± 0.500	
51244.681500	-49.145 ± 0.500	-45.191 ± 0.500	
51452.415900	-51.065 ± 0.040	-43.414 ± 0.050	
51502.257600	-51.429 ± 0.050	-43.378 ± 0.050	
51648.640100	-51.951 ± 0.050	-42.621 ± 0.050	
51717.538800	-51.956 ± 0.050	-42.274 ± 0.050	

Table 8. Radial-velocity measurements of GI 747. To be published in electronic form only.

GI831AB

Julian Day 2400000+	V_A (in km/s)	V_B (in km/s)	References
			this paper
49977.4017	$-58.778 \pm .100$	-53.553 ± 1.000	
50313.4914	$-55.660 \pm .500$		
50386.2936	$-51.831 \pm .100$	-61.573 ± 1.000	
50420.2883	$-49.608 \pm .100$	-69.171 ± 2.000	
50642.5675	$-57.856 \pm .100$	-53.964 ± 1.000	
50673.5155	$-58.450 \pm .100$	-52.600 ± 1.000	
50746.2883	$-59.194 \pm .100$	-52.852 ± 1.000	
50983.5875	$-56.364 \pm .500$		
51019.5585	$-55.788 \pm .500$		
51109.3370	$-50.642 \pm .050$	$-65.978 \pm .500$	
51162.2405	$-48.499 \pm .100$	-72.198 ± 1.000	
51163.2380	$-48.772 \pm .100$	-70.663 ± 1.000	
51364.5670	$-57.635 \pm .500$		
51396.5163	$-58.358 \pm .500$		
51451.3961	$-58.683 \pm .500$		

Table 9. Radial-velocity measurements of GI 831. To be published in electronic form only.

Gl866ABC

Julian Day 2400000+	V_A (in km/s)	V_B (in km/s)	V_C (in km/s)	References
50019.325	$-25.004 \pm .100$	$-53.301 \pm .080$	$-77.626 \pm .300$	Delfosse et al. 1999b
50313.543	$-79.960 \pm .100$	$-46.680 \pm .120$		
50386.336	$-38.987 \pm .100$			
50389.319	$-76.516 \pm .100$	$-50.815 \pm .080$	$-15.680 \pm .500$	
50418.269	$-46.732 \pm .700$			
50419.244	$-81.252 \pm .100$	$-52.148 \pm .100$		
50419.324	$-80.921 \pm .100$	$-51.979 \pm .080$		
50420.249	-47.177 ± 1.000			
50641.595	$-40.094 \pm .100$	$-56.016 \pm .070$		
50642.594	$-78.992 \pm .300$	$-55.744 \pm .120$		
50643.596	$-47.563 \pm .300$			
50644.594	$-14.713 \pm .100$	$-55.855 \pm .070$		
50645.598	-50.656 ± 1.000			
50646.592	$-78.420 \pm .100$	$-55.849 \pm .100$	$-7.567 \pm .400$	
50647.605	$-35.530 \pm .300$			
50672.583	$-72.725 \pm .110$	$-56.314 \pm .110$		
50673.471	$-67.182 \pm .200$		$-19.782 \pm .300$	
50674.617	$-17.102 \pm .100$	$-56.341 \pm .060$		
50976.890	-54.268 ± 1.000	$-37.044 \pm .100$		
50998.903	$-85.950 \pm .300$	$-35.550 \pm .100$	$-23.400 \pm .500$	
51020.847	$-80.600 \pm .500$	$-35.700 \pm .200$	$-30.000 \pm .500$	
51068.673	$-23.183 \pm .100$	$-40.454 \pm .100$		
51017.580	$-89.724 \pm .080$	$-35.289 \pm .100$		
51108.353	$-85.172 \pm .050$	$-44.530 \pm .050$	$-13.116 \pm .200$	
51159.238	$-22.522 \pm .200$	$-48.651 \pm .200$		
51161.231	$-81.280 \pm .200$	$-48.331 \pm .200$		
51363.594	$-22.324 \pm .070$	$-55.070 \pm .090$	$-79.100 \pm .310$	

Table 10. Radial-velocity measurements of Gl 866ABC. To be published in electronic form only.

Gl234AB

Julian Day 2400000+	ρ (arc sec)	θ (degree)	Method	References
35189.500	$1.190 \pm .050$	36.0 ± 5.0	photograph	Probst et al. 1977
35545.500	$1.160 \pm .050$	43.2 ± 5.0	visual	Probst et al. 1977
35942.500	$1.220 \pm .050$	51.9 ± 5.0	visual	Probst et al. 1977
42063.500	$1.270 \pm .050$	53.0 ± 40.0	photoelec	Probst et al. 1977
46778.500	$1.110 \pm .110$	22.6 ± 2.0	speckle	Coppenbarger et al. 1994
48583.500	$1.190 \pm .048$	66.0 ± 2.0	speckle	Coppenbarger et al. 1994
48673.500	$1.100 \pm .044$	66.3 ± 2.0	speckle	Coppenbarger et al. 1994
51506.080	$.457 \pm .001$	$270.4 \pm .1$	A.O.	this paper
51592.900	$.439 \pm .0005$	$287.4 \pm .1$	A.O.	this paper
51655.315	$.444 \pm .001$	$299.7 \pm .1$	A.O.	this paper
	Position Angle	Projected separations		
46368.500	$1.040 \pm .100$.0	speckle	Coppenbarger et al. 1994
47107.500	$1.120 \pm .110$.0	speckle	Coppenbarger et al. 1994
47198.500	$.980 \pm .090$	90.0	speckle	Coppenbarger et al. 1994
47576.500	$.810 \pm .080$	90.0	speckle	Coppenbarger et al. 1994

Table 11. Angular separation measurements for Gl 234AB. To be published in electronic form only.

G1644A-BC

Julian Day 2400000+	ρ (arc sec)	θ (degree)	Type	References
45863.690	.230 \pm .020	115.4 \pm 5.0	speckle	Al Shukri et al. 1996
45864.603	.243 \pm .030	115.1 \pm 5.0	speckle	Al Shukri et al. 1996
46592.937	.197 \pm .011	48.5 \pm 2.5	speckle	Blazit et al. 1987
46593.960	.208 \pm .006	41.3 \pm 1.5	speckle	Blazit et al. 1987
46934.452	.242 \pm .010	206.9 \pm 2.0	speckle	Balega et al. 1989
47260.554	.213 \pm .010	16.9 \pm 2.0	speckle	Balega et al. 1991
47676.373	.240 \pm .015	143.8 \pm 5.0	speckle	Balega et al. 1994
48378.066	.211 \pm .010	102.7 \pm 3.0	speckle	Hartkopf et al. 1994
51017.500	.216 \pm .002	21.9 \pm .3	A.O.	this paper
51414.780	.231.2 \pm .0005	161.5 \pm .1	A.O.	this paper
51594.128	.207.7 \pm .0005	53.6 \pm .1	A.O.	this paper
51650.080	.213 \pm .001	18.3 \pm .2	A.O.	this paper
51717.956	.216 \pm .004	340.3 \pm 1.0	A.O.	this paper

Table 12. Angular separation measurements for G1644A-BC. To be published in electronic form only.

G1747AB

Julian Day 2400000+	ρ (arc sec)	θ (degree)	Type	References
46596.005	.148 \pm .010	110.6 \pm 3.9	speckle	Blazit et al. 1987
46580.446	.147 \pm .010	110.6 \pm 3.9	speckle	Balega et al. 1989
46669.309	.089 \pm .010	117.4 \pm 6.4	speckle	Balega et al. 1989
46934.525	.141 \pm .010	233.0 \pm 4.1	speckle	Balega et al. 1989
51413.815	.304 \pm .004	256.1 \pm .1	A.O.	this paper
51414.815	.298 \pm .001	255.9 \pm .1	A.O.	this paper
51508.191	.331 \pm .001	258.6 \pm .1	A.O.	this paper
51645.119	.3542 \pm .0004	262.3 \pm .1	A.O.	this paper

Table 13. Angular separation measurements for G1 747AB. To be published in electronic form only.

G1831AB

Julian Day 2400000+	ρ (arc sec)	θ (degree)	Type	References
51414.925	.187 \pm .002	134.4 \pm .4	A.O.	this paper
51507.700	.198 \pm .001	149.4 \pm .2	A.O.	this paper
51715.091	.109 \pm .004	203.1 \pm .4	A.O.	this paper

Table 14. Angular separation measurements for G1 831AB. To be published in electronic form only.

Gl866AC-B

Julian Day 2400000+	X (arc sec)	Y (arc sec)	Type	References
46381.500	.400 ± .020	.000 ± .020	speckle	Leinert et al. 1990
46385.500	.390 ± .020	.000 ± .020	speckle	Leinert et al. 1990
46594.500	.435 ± .010	-.165 ± .010	speckle	Leinert et al. 1990
46603.500	.440 ± .010	-.165 ± .010	speckle	Leinert et al. 1990
46686.500	.275 ± .020	-.200 ± .020	speckle	Leinert et al. 1990
46690.500	.280 ± .020	-.175 ± .020	speckle	Leinert et al. 1990
46952.500	-.105 ± .025	.105 ± .025	speckle	Leinert et al. 1990
46954.500		.110 ± .020	speckle	Leinert et al. 1990
46962.500	-.085 ± .010	.130 ± .010	speckle	Leinert et al. 1990
47044.500	.120 ± .020	.085 ± .020	speckle	Leinert et al. 1990
47048.500	.125 ± .020	.100 ± .020	speckle	Leinert et al. 1990
47107.500	.290 ± .020		speckle	Leinert et al. 1990
47165.500	.375 ± .020	.020 ± .020	speckle	Leinert et al. 1990
47339.500	.445 ± .030	-.085 ± .030	speckle	Leinert et al. 1990
47410.500	.440 ± .025	-.175 ± .025	speckle	Leinert et al. 1990
	ρ (arc sec)	θ (degree)		
48136.518	.481 ± .018	348.0± 2.2	speckle	Woitas et al. 2000
48230.495	.463 ± .019	339.8± 2.4	speckle	Woitas et al. 2000
48559.482	.200 ± .013	155.5± 3.8	speckle	Woitas et al. 2000
48759.502	.244 ± .006	15.3± .5	speckle	Woitas et al. 2000
48910.493	.449 ± .011	350.8± 1.5	speckle	Woitas et al. 2000
48998.471	.480 ± .012	348.6± 1.4	speckle	Woitas et al. 2000
49198.514	.259 ± .011	319.3± 1.2	speckle	Woitas et al. 2000
49263.491	.105 ± .004	277.7± .5	speckle	Woitas et al. 2000
49474.505	.126 ± .004	74.9± 2.7	speckle	Woitas et al. 2000
49610.484	.327 ± .004	5.9± .4	speckle	Woitas et al. 2000
49699.494	.434 ± .004	354.0± .2	speckle	Woitas et al. 2000
49700.516	.439 ± .004	354.3± .3	speckle	Woitas et al. 2000
49908.462	.439 ± .004	337.3± .3	speckle	Woitas et al. 2000
49946.521	.392 ± .004	333.1± .3	speckle	Woitas et al. 2000
50243.513	.156 ± .003	131.6± 1.1	HST FGS3	Woitas et al. 2000
50354.473	.188 ± .004	28.0± .5	speckle	Woitas et al. 2000
50625.500	.488 ± .007	345.8± 1.7	HST Planetary Camera	Schroeder et al. 2000
50656.500	.486 ± .007	343.8± 1.7	HST Planetary Camera	Schroeder et al. 2000
50686.506	.485 ± .004	340.2± .2	speckle	Woitas et al. 2000
50769.489	.391 ± .004	333.3± .1	speckle	Woitas et al. 2000
50941.495	.104 ± .007	214.8± .3	speckle	Woitas et al. 2000
51017.500	.200 ± .003	155.9 ± .9	A.O.	this paper
51017.500	.198 ± .003	156.2± .9	A.O.	this paper
51097.490	.133 ± .004	101.2± .2	speckle	Woitas et al. 2000
51414.925	.480 ± .001	348.4± .1	A.O.	this paper
51507.725	.473 ± .001	341.0± .1	A.O.	this paper

Table 15. angular measurements for Gl866AC-B. To be published in electronic form only.